EM-ANN MODELING AND OPTIMAL CHAMFERING OF 90° CPW BENDS WITH AIR-BRIDGES

P.M. Watson and K.C. Gupta

Center for Advanced Manufacturing and Packaging of Microwave, Optical, and Digital Electronics (CAMPmode)
and
Department of Electrical and Computer Engineering
University of Colorado at Boulder
Boulder, CO 80309-0425

Abstract **--** Electromagnetically-trained artificial neural network (EM-ANN) models for coplanar waveguide (CPW) 90° bends with air-bridges are presented. The optimal chamfer is determined for a conventional CPW bend where both the slot and strip are chamfered. Also, a novel compensated CPW bend is introduced where only the strip is chamfered. Optimum value of this chamfer is found to be the maximum chamfer allowed by air-bridge placement. This novel compensated CPW bend is shown to reduce the return loss from that in the conventional optimally chamfered CPW bend by 3 to 7 dB.

I. Introduction

Recently, coplanar waveguide (CPW) MMICs have attracted much attention due to several advantages offered by CPW configuration, such as the ease of shunt and series connections, the low radiation, the low dispersion, and the avoidance of thin fragile substrates. Currently, design software available for CPW circuits is inadequate because of non-availability of accurate and efficient models for CPW discontinuities such as bend, T-junctions, step-in-impedance, short and open stubs, etc. We have derived EM-ANN models for CPW components suitable for use in MMIC design. This paper is focused on CPW bends. Other models (CPW line parameters, short circuit, T-junction, step-in-width, etc.) developed will be presented at the Symposium.

Earlier work on CPW bend characterization has been described in [1-8]. Air-bridges are placed near CPW discontinuities in order to reduce the unwanted slot-line mode which tends to radiate [9]. The slot-line mode is generated in CPW bends due to the path length difference of the slots. The inclusion of air-bridges, however, adds unwanted capacitance which degrades the performance of the bend. In addition to compensating for the reactances associated with the bend, chamfering provides a simple

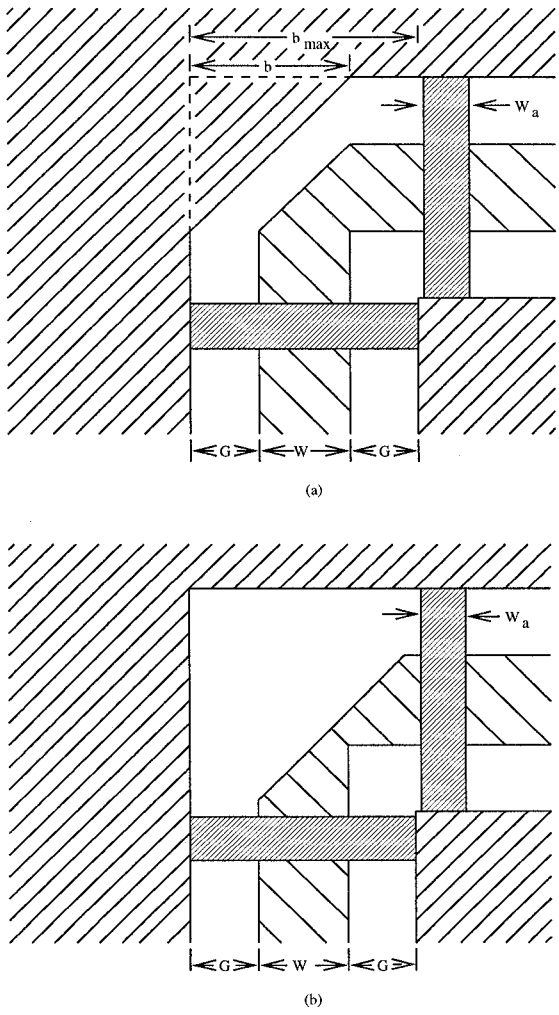

Fig. 1 CPW 90° bend structures with W_a = 40 μm, H_a = 3μm, H_{sub} = 625 μm, ε_r = 12.9, and tanδ = 0.0005. (a) Conventional chamfered bend and (b) novel compensated bend (H_a is height of air-bridge above the substrate, and H_{sub} is the substrate thickness.)

0-7803-4603-6/97/$5.00 (c) IEEE

way to partially compensate for the effects of the air-bridges. The work described in this paper investigates the effects of chamfering on the S-parameters for the CPW 90° bends shown in Fig. 1a,b. Optimal chamfering values are determined for the different bend structures.

CPW bends of the type shown in Fig. 1a have been studied in [3] for b=0 and b=W+G. The work reported in [3] is extended upon by determining the optimal chamfer for each bend structure. The compensated CPW bend shown in Fig. 1b is a novel structure which has been shown, by EM simulation, to improve upon the return loss and the insertion loss of the conventional chamfered bend of Fig. 1a. Electromagnetically-trained artificial neural network (EM-ANN) models are developed for the CPW bends and are used to determine optimal chamfer values. Details of EM-ANN modeling methodology have previously been presented in [10,11]. In this work, all air-bridge parameters are held constant in order to concentrate on the effects caused by the chamfering of the bends.

II. Optimally Chamfered Conventional CPW Bend

An EM-ANN model has been developed for the CPW bend structure shown in Fig. 1a. Variable inputs for the EM-ANN model are W, G, b/b_{max}, and frequency. Model outputs are S-parameters. Substrate material used is GaAs, and the thickness is 625 μm for all results included in this paper. Air-bridges are 40 μm wide (W_a), 3 μm (H_a) above the GaAs surface, and are positioned at the bend discontinuity as shown. Note, all air-bridge parameters are held constant in order to concentrate on the effects caused by the chamfering of the bends.

EM simulations were performed on 17 bend structures, included within the range of parameters given in Table 1, using *Momentum*[*] [12].

Table 1 Variable parameter ranges for CPW components.

	Min.	Max.
Frequency	1 GHz	50 GHz
W	20 μm	120 μm
G	20 μm	60 μm

Characteristic impedances used for port terminations have been determined from *linecalc*[*] [13]. Five different values of chamfer were simulated for each bend, with b/b_{max} ranging from 0 to 1. The strip corner was chamfered by a proportional amount given by bW/(W+G). EM simulation data was separated into training, testing, and verification data sets for model development. Error results (EM-ANN model compared to EM simulation) are shown in Table 2.

Table2 Error results (average and standard deviation) for the optimally chamfered CPW bend. (Verification dataset)

	|S11|	∠S11(°)	|S21|	∠S21(°)
avg. error	0.000966	0.123805	0.000354	0.047837
Std. Dev.	0.001058	0.140618	0.000339	0.039378

It was determined that indeed there exists an optimal chamfer for each structure, especially when analyzing the return loss, $20\log|S_{11}|$. The developed EM-ANN model can reproduce the trends in S-parameters determined by the changes in the physical structure of the CPW bend. Using this model, the optimal chamfer for each bend is determined. Fig. 2 shows the optimal chamfer, b/b_{max}, versus W/G for minimum return loss, as determined by the EM-ANN model. The optimal chamfer as a function of W/G is given by

$$b/b_{max} = 0.2102 \ln(W/G) + 0.7677 \quad \text{for } 0 \le W/G \le 2.5 \quad (1)$$
$$= 1 \quad \text{for } W/G > 2.5$$

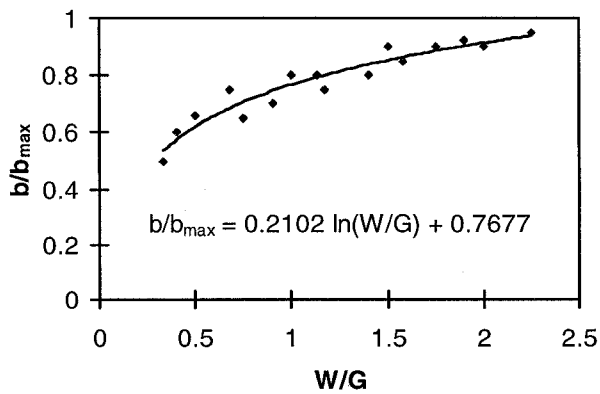

Fig. 2 Optimal chamfer for return loss versus W/G for the conventional bend of Fig. 1a.

[*] A tradename of HP-EEsof software product

III. Novel Compensated CPW Bend

An EM-ANN model has been developed for the novel compensated CPW bend structure, proposed here, shown in Fig. 1b. This novel bend is capable of improving upon the performance of the already discussed optimally chamfered CPW bend. Variable input parameters for the model are W, G, and frequency. Model outputs are S-parameters. For this novel bend, the optimum chamfer for the strip is found to be the maximum allowable by air-bridge placement. EM simulations have been performed on 17 bend structures, included within the range of parameters given in Table 1, to provide training, testing, and verification data. Error results for the developed EM-ANN model are shown in Table 3.

Table 3 Error results (average and standard deviation) for the compensated bend model. (Verification dataset)

	$\|S_{11}\|$	$\angle S_{11}$	$\|S_{21}\|$	$\angle S_{21}$
Avg. Err.	0.00139	1.020°	0.00071	0.447°
Std. Dev.	0.00086	0.759°	0.00037	0.380°

IV. CPW Bend Comparisons

The novel compensated CPW bend structure is found to improve the return loss over the optimally chamfered conventional bend, as shown in Table 4. We believe this to be due to a decrease in capacitance as the slot width at the corner is increased, thereby compensating for the increase in capacitance due to the air-bridges. Improvements are also seen in the insertion loss. Note that all air-bridge parameters remain the same as in the case for the optimally chamfered CPW bend.

Comparisons between unchamfered CPW corner, optimally chamfered conventional bend, and the novel compensated bends are shown in Fig. 3 for CPW bend structures with W= 70 μm and G= 20 μm, corresponding to Z_o=35 Ω. Note that all air-bridges and reference planes are at the same positions. Based on the results shown in Fig. 3 and in Table 4, the new compensated bend provides significant improvements in return and insertion loss over the other CPW bend structures. Improvements are also seen when comparing the optimally chamfered bend results to the corner (unchamfered) bend.

Table 4 Comparison of return loss for the conventional optimally chamfered bend and the novel compensated bend for several structures. (Frequency = 50 GHz)

W (μm)	G (μm)	Optimally Chamfered bend Return loss (dB)	Novel bend Return loss (dB)	Improvement (dB)
70	60	-13.89	-20.92	7.03
120	40	-12.96	-16.36	3.40
70	20	-21.51	-26.94	5.43
35	55	-17.27	-20.18	2.91
105	55	-12.50	-17.02	4.52
105	25	-15.76	-19.33	3.57
70	40	-16.36	-21.41	5.05

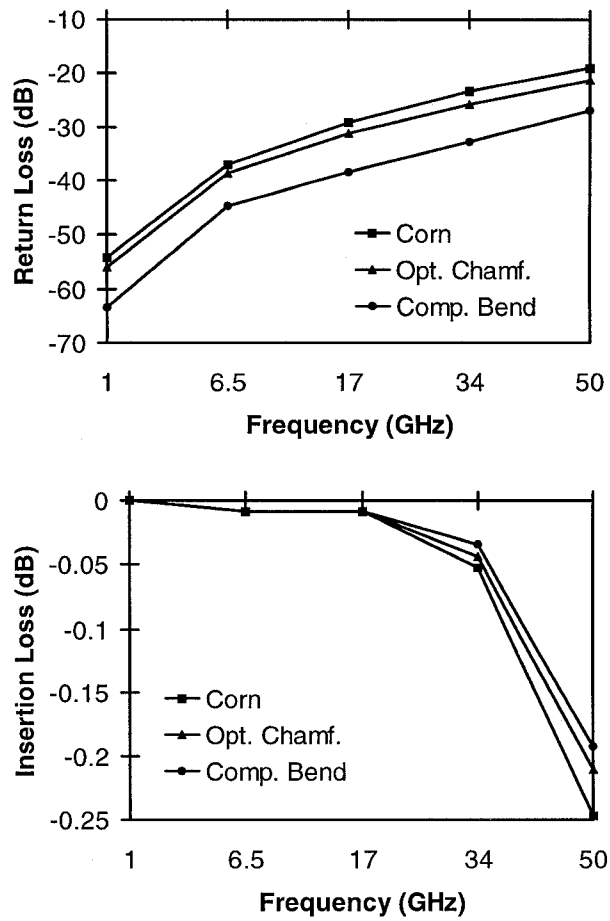

Fig. 3 Comparison of unchamfered (Corn), conventional (Opt. Chamf.), and novel (Comp. Bend) CPW bends. W= 70 μm and G=20 μm.

V. Concluding Remarks

EM-ANN models have been developed for optimally chamfered CPW 90° bends and a novel compensated CPW 90° bend. It has been shown that chamfering the corner of 90° CPW bends provides a simple way to improve their performance. The optimal chamfer for a conventional CPW bend, where both the slot and strip corners are chamfered, has been determined. A novel compensated CPW bend structure, where only the strip is chamfered, has been introduced and shown to provide improved performance over the optimally chamfered conventional CPW bend. Chamfering the inside corner of the ground plane of any of the CPW bends (as shown in Fig. 4) did not improve their performance.

EM-ANN models have also been developed for CPW frequency dependent line parameters, CPW short circuits, and CPW symmetric T-junctions. EM-ANN models are also being developed for open circuit stubs and step-in-width, etc.

These models are easily inserted into a commercial microwave simulator where they provide accuracy approaching that of the EM simulation tool used for developing the components' models. Design of CPW circuits such as filters, power dividers, and matching networks using the EM-ANN models will be demonstrated at the Symposium.

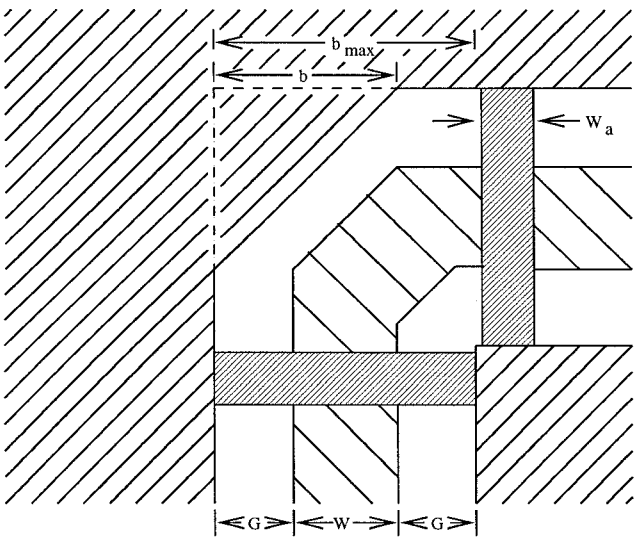

Fig. 4 CPW 90° bend with inside slot corner chamfered.

References

[1] M. Wu et al., "Full-Wave Characterization of the Mode Conversion in a CPW Right-Angled Bend," *IEEE Trans. on Microwave Theory and Techniques,* Vol. 43, No. 11, pp. 2532-2538, Nov. 1995.

[2] T. Becks and I. Wolff, "Full-Wave Analysis of Various CPW Bends and T-junctions with Respect to Different Types of Air-Bridges," *MTT-S Int. Microwave Symp. Dig.,* 1993, pp. 697-700.

[3] A.A. Omar et al., "Effects of Air-bridges and Mitering on CPW 90° Bends: Theory and Experiment," *MTT-S Int. Microwave Symp. Dig.,* 1993, pp. 823-826.

[4] C. Sinclair et al., "Closed-Form Expressions for CPW Discontinuities," *Conference Proceedings: Military Microwaves 92,* pp. 227-229.

[5] S. Alexandrou et al., "Time-Domain Characterization of Bent CPWs," *IEEE Journal of Quantum Electronics,* Vol. 28, No. 10, pp. 2325-32, Oct. 1992.

[6] R. Bromme and R.H. Jansen, "Systematic Investigation of CPW MIC/MMIC Structures using a Unified Strip/Slot 3D EM Simulator," *MTT-S Int. Microwave Symp. Dig.,* 1991, pp. 1081-4.

[7] H. Sawasa et al., "Transmission Characteristics of CPW Bends for Various Curvatures," *IEICE Transactions on Electronics,* Vol. E77-C, No. 6, pp. 949-51, Jun. 1994.

[8] H. Sawasa et al, "Radiation from Bend in CPW Angular and Circular Bends," *1994 Int. Symp. on EM Comp.,* p. 325.

[9] M. Riaziat et al., "Coplanar Waveguides used in 2-18 GHz Distributed Amplifier," *MTT-S Int. Microwave Symp. Dig.,* 1986, pp. 337-338.

[10] P. Watson and K.C. Gupta, "EM-ANN Models for Via Interconnects in Microstrip Circuits," *MTT-S Int. Microwave Symp. Dig.*, 1996, pp. 1819-1822.

[11] P.M. Watson and K.C. Gupta, "EM-ANN Models for Microstrip Vias and Interconnects in Multilayer Circuits," *IEEE Trans. on Microwave Theory and Tech.,* Vol. 44, No. 12, Dec. 1996, pp. 2495-2503.

[12] *Momentum,* ver. A.02.00, Hewlett-Packard Co., Santa Rosa, CA., 1995.

[13] *linecalc*, ver. 5.0, Hewlett-Packard Co., Santa Rosa, CA., 1994.